Stationary Light Pulses in Cold Atomic Media and without Bragg Gratings

Yen-Wei Lin, Wen-Te Liao, Thorsten Peters, Hung-Chih Chou, Jian-Siung Wang, Hung-Wen Cho, Pei-Chen Kuan, and Ite A. Yu*

Department of Physics, National Tsing Hua University, Hsinchu 30013, Taiwan, Republic of China

(Received 18 February 2009; published 28 May 2009)

We study the creation of stationary light pulses (SLPs), i.e., light pulses without motion, based on the effect of electromagnetically induced transparency with two counterpropagating coupling fields in cold atoms. We show that the Raman excitations created by counterpropagating probe and coupling fields prohibit the formation of SLPs in media of cold and stationary atoms such as laser-cooled atom clouds, Bose condensates or color-center crystals. A method is experimentally demonstrated to suppress these Raman excitations and SLPs are realized in laser-cooled atoms. Furthermore, we report the first experimental observation of a bichromatic SLP at wavelengths for which no Bragg grating can be established. Our work advances the understanding of SLPs and opens a new avenue to SLP studies for few-photon nonlinear interactions.

DOI: 10.1103/PhysRevLett.102.213601 PACS numbers: 42.50.Gy, 32.80.Qk

Applications based on electromagnetically induced transparency (EIT) [1], such as slow light and storage and retrieval of light pulses provide a coherent way to transfer a quantum state between light and matter [2–4]. They are therefore considered as promising tools for future quantum networks. One requirement for such use, however, the strong interaction between few-photon light pulses, is so far most efficiently achievable in cavity quantum electrodynamics [5]. Some years ago Bajcsy *et al.* demonstrated the formation of stationary light pulses (SLPs) based on a counterpropagating EIT scheme in a hot gaseous atomic medium [6]. As SLPs significantly increase the interaction time between media and light while maintaining an electromagnetic component unlike stored light pulses, they are very promising for low-light-level nonlinear optics and quantum information processing.

To our knowledge, no further experimental data exist demonstrating the formation of SLPs so far, especially not in media of cold or stationary atoms such as laser-cooled atoms, Bose condensates, or color-center crystals. The SLP phenomenon has been studied theoretically in the case of stationary atomic media [7]. The authors came to the conclusion, that SLPs can be created in such media. In this Letter, we point out that counterpropagating Raman excitations exist between the forward and backward fields which prohibit a SLP formation in media of cold or stationary atoms. For hot gaseous media these Raman excitations can be neglected. We experimentally demonstrate a solution to suppress these counterpropagating Raman excitations and realize SLPs in laser-cooled atoms.

In the first experimental realization of SLPs in Ref. [6], the underlying mechanism of SLPs was identified as a band gap being created by a Bragg grating due to a standing-wave coupling field. Theoretical work by Moiseev and Ham [8,9] introduced a model where SLPs can be understood as the result of multiwave mixing (MWM) processes. To demonstrate that a Bragg grating is not necessary for the creation of SLPs, we report the first experimental observation of a bichromatic SLP at wavelengths for which no Bragg grating can be established, supporting the MWM model of SLPs.

Consider a three-level system with two metastable ground states $|1\rangle$ and $|2\rangle$ and an excited state $|3\rangle$ with decay rate Γ. The probe and coupling fields drive the $|1\rangle \leftrightarrow |3\rangle$ and $|2\rangle \leftrightarrow |3\rangle$ transitions resonantly with Rabi frequencies Ω_p and Ω_c, respectively, [see Fig. 1(a)]. The following equations are widely used in the studies of EIT, slow light, and storage of light [10]

$$\frac{\partial \rho_{31}}{\partial t} = \frac{i}{2}\Omega_p + \frac{i}{2}\Omega_c \rho_{21} - \frac{\Gamma}{2}\rho_{31}, \tag{1}$$

$$\frac{\partial \rho_{21}}{\partial t} = \frac{i}{2}\Omega_c^* \rho_{31} - \gamma \rho_{21}, \tag{2}$$

$$\frac{1}{c}\frac{\partial \Omega_p}{\partial t} + \frac{\partial \Omega_p}{\partial z} = i\frac{\alpha\Gamma}{2L}\rho_{31}. \tag{3}$$

Here γ is the ground-state relaxation rate and α and L are the optical density and the length of the medium, respectively. In the case of forward- and backward-propagating probe pulses and coupling fields as needed for the creation of SLPs, we replace Ω_c, Ω_p, ρ_{31}, and ρ_{21} by $\Omega_c^+ e^{ikz} + \Omega_c^- e^{-ikz}$, $\Omega_p^+ e^{ikz} + \Omega_p^- e^{-ikz}$, $\rho_{31}^+ e^{ikz} + \rho_{31}^- e^{-ikz}$, and $\rho_{21}^0 + \rho_{21}^{+-} e^{-2ikz} + \rho_{21}^{-+} e^{2ikz}$, respectively. Here, k indicates the wave vector and we assume that the probe and coupling wavelengths are nearly the same. By neglecting terms containing e^{inkz} with $n > 2$, we finally obtain the following equations:

$$\frac{\partial \rho_{31}^+}{\partial t} = \frac{i}{2}\Omega_p^+ + \frac{i}{2}(\Omega_c^+ \rho_{21}^0 + \Omega_c^- \rho_{21}^{-+}) - \frac{\Gamma}{2}\rho_{31}^+, \tag{4}$$

$$\frac{\partial \rho_{31}^-}{\partial t} = \frac{i}{2}\Omega_p^- + \frac{i}{2}(\Omega_c^- \rho_{21}^0 + \Omega_c^+ \rho_{21}^{+-}) - \frac{\Gamma}{2}\rho_{31}^-, \tag{5}$$

$$\frac{\partial \rho_{21}^{+-}}{\partial t} = \frac{i}{2}(\Omega_c^+)^* \rho_{31}^- - \gamma_2 \rho_{21}^{+-}, \tag{6}$$

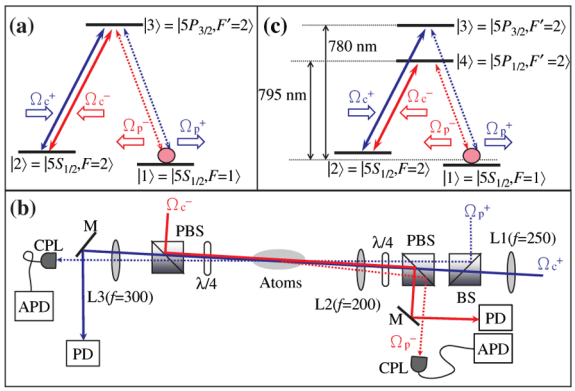

FIG. 1 (color online). (a) and (c) Relevant energy levels and laser excitations in the experiments. (b) Schematic experimental setup. BS: beam splitter cube; PBS: polarizing beam splitter cube; $\lambda/4$: quarter-wavse plate; L1-L3: lenses (f indicates the focal length in units of mm); CPL: optical fiber coupler; M: mirror; PD: photo detector; APD: avalanche photo detector. L2 focused the probe beam onto the atom cloud. L1 transformed the coupling beam into a plane wave in the region of the atom cloud. L3 collimated the transmitted probe beam.

$$\frac{\partial \rho_{21}^{-+}}{\partial t} = \frac{i}{2}(\Omega_c^-)^* \rho_{31}^+ - \gamma_2 \rho_{21}^{-+}, \tag{7}$$

$$\frac{\partial \rho_{21}^{0}}{\partial t} = \frac{i}{2}[(\Omega_c^+)^* \rho_{31}^+ + (\Omega_c^-)^* \rho_{31}^-] - \gamma_1 \rho_{21}^{0}, \tag{8}$$

$$\frac{1}{c}\frac{\partial \Omega_p^+}{\partial t} + \frac{\partial \Omega_p^+}{\partial z} = i\frac{\alpha\Gamma}{2L}\rho_{31}^+, \tag{9}$$

$$\frac{1}{c}\frac{\partial \Omega_p^-}{\partial t} - \frac{\partial \Omega_p^-}{\partial z} = i\frac{\alpha\Gamma}{2L}\rho_{31}^-. \tag{10}$$

While ρ_{21}^0, created by the copropagating coupling and probe fields, varies spatially on the order of millimeters, $\rho_{21}^{+-} e^{-2ikz}$ and $\rho_{21}^{-+} e^{2ikz}$ created by the counterpropagating fields vary with a period of half the laser wavelength, i.e., several hundred nanometers. The atomic motion causes little relaxation on ρ_{21}^0 but a much larger relaxation on $\rho_{21}^{+-} e^{-2ikz}$ and $\rho_{21}^{-+} e^{2ikz}$. Therefore we introduce two relaxation rates γ_1 and γ_2 (with $\gamma_2 \geq \gamma_1$) to represent the different decay of ρ_{21}^0 and ρ_{21}^{+-} (as well as ρ_{21}^{-+}), respectively. The relaxation rate γ_1 is in our case dominated by inhomogeneous magnetic fields present in the experimental system. The relaxation rate γ_2, however, should be mainly determined by dephasing due to atomic motion.

In room-temperature or hot media, atoms move fast and γ_2 is very large such that ρ_{21}^{+-} and ρ_{21}^{-+} are negligible. Figure 2(b) shows the numerical result for the probe pulse intensity when a SLP in a hot medium is formed by setting $\rho_{21}^{+-} \equiv 0 \equiv \rho_{21}^{-+}$. The probe pulse first moves through the medium in the presence of only the forward coupling field. At $t = 80\Gamma^{-1}$, the coupling field is switched off to store the probe pulse. At $t = 110\Gamma^{-1}$, both forward and backward coupling fields are simultaneously turned on and a SLP is established.

In cold media ρ_{21}^{+-} and ρ_{21}^{-+} should not be neglected; i.e., $\gamma_2 \ll \Gamma$ must be allowed. Figure 2(c) shows the numerical result calculated with Eqs. (4)–(10) for a medium of cold atoms with the same calculation parameters as in Fig. 2(b), except now $\gamma_2 = 0$. As both coupling fields of equal intensity are turned on simultaneously at $t = 110\Gamma^{-1}$, no SLP is formed. Instead, the probe pulse splits up into two counterpropagating pulses of equal amplitude. This effect due to the Raman excitations contained in Eqs. (4)–(8) is illustrated in Fig. 3. Figures 3(a) and 3(b) show the Raman excitations driven by copropagating coupling and probe fields and Figs. 3(c) and 3(d) show the excitations driven by counterpropagating fields. These two counterpropagating Raman excitations have only to be considered for cold media where, e.g., they allow us to perform slow light experiments with counterpropagating probe and coupling fields. As can be seen from Fig. 2(c), such counterpropagating excitations prohibit the formation of SLPs.

To prevent excitation of the two counterpropagating processes, γ_2 could be increased in order to make ρ_{21}^{+-} and ρ_{21}^{-+} negligible. However, γ_2 is mainly determined by the atom temperature and is not easily modified without changing other experimental parameters. A more simple and efficient way to prevent the hybrid excitations is to apply a detuning Δ between the forward and backward coupling frequencies. Because the forward- and backward-propagating probe fields are retrieved by the forward and backward coupling fields, respectively, the Raman excitations shown in Figs. 3(a) and 3(b) are still two-photon resonant and provide the dominant contribution to the probe pulse propagation. On the other hand, the two counterpropagating processes shown in Figs. 3(c) and 3(d) can be considered not two-photon resonant if the detuning is much larger than the width of the EIT transparency win-

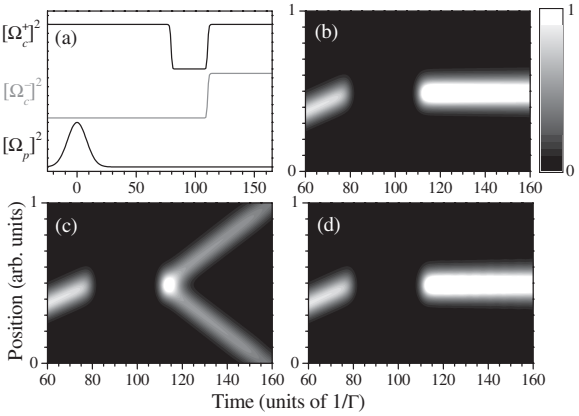

FIG. 2. Numerical simulations of the probe intensity ($|\Omega_p^+|^2 + |\Omega_p^-|^2$) as a function of time and position for the timing sequence depicted in (a). The gray level indicates the amplitude. In (b), a medium of hot atoms is considered with $\rho_{21}^{+-} \equiv 0 \equiv \rho_{21}^{-+}$. In (c) and (d), a medium of cold atoms is considered with $\gamma_2 = 0$. The detunings are $\Delta = 0$ (c) and 1.0Γ (d). The other parameters common to all plots are $\alpha = 2000$, $\Omega_c^{\pm} = 3.5\Gamma$, and $\gamma_1 = 0$.

dow, i.e., $\Delta \gg (\Omega_c^2/\Gamma)(1/\alpha)$, where Ω_c^2/Γ is the width of the EIT transparency window in the low-OD limit and a large OD ($\alpha \gg 1$) further narrows the width. In this case, the counterpropagating processes are negligible. With a detuning Δ applied between the coupling fields, we make the following revisions to Eqs. (5)–(7), respectively:

$$\frac{\Gamma}{2} \rightarrow \frac{\Gamma}{2} - i\Delta, \qquad \gamma_2 \rightarrow \gamma_2 - i\Delta, \qquad \gamma_2 \rightarrow \gamma_2 + i\Delta. \tag{11}$$

Calculated with $\Delta = 1.0\Gamma$ [all other parameters as in Fig. 2(c)], Fig. 2(d) shows that a SLP is now formed in a cold medium. The comparison of Figs. 2(b) and 2(d) shows almost no quantitative difference; i.e., hot and cold media behave the same for SLPs when a detuning between the coupling fields is applied.

To show the validity of the previous theoretical discussion we performed experiments in a cloud of cold ^{87}Rb atoms produced by a magneto-optical trap (MOT) [11]. There were 1.1×10^9 atoms in the MOT. Figures 1(a) and 1(b) show the laser excitations and the experimental setup. All laser fields were circularly polarized (σ^+). The two counterpropagating coupling beams had a e^{-2} full width of 6.0 mm and interacted with all trapped atoms. The incident probe beam was focused to a e^{-2} full width of 0.27 mm and propagated along the major axis of the cigar-shaped atom cloud. The probe and coupling beams intersected at an angle of about 0.3°. Two avalanche photo detectors (APD, Hamamatsu C5460, rise time 36 ns) detected the probe transmissions in the forward and backward directions simultaneously. After propagating through the atoms, the two coupling beams were blocked in order to reduce their influence on the two APDs. Parts of the forward- and backward-propagating probe beams were also blocked and the collection efficiencies of the two APDs were different. More experimental details can be found in Ref. [12]. The experimental values of the optical density α, the coupling Rabi frequencies $\Omega_c^{\pm}$ and the ground-state relaxation rate γ_1 were determined by adjusting the parameters of the numerical simulation until its results reproduced the experimental data of the probe transmission well as shown in Figs. 4(a) and 4(b). The relaxation rate γ_2 was determined similarly for counterpropagating probe and coupling fields as shown in Fig. 4(c).

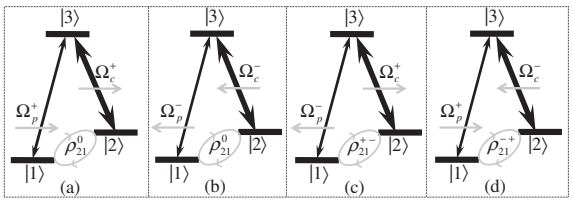

FIG. 3. The four Raman excitations that describe the interaction between the two light fields and media of cold atoms. For hot media, only the copropagating Raman excitations in (a) and (b) need to be considered and the counterpropagating Raman excitations in (c) and (d) are negligible.

Figure 4(d) shows the theoretical prediction of a SLP created in a hot medium calculated with $\rho_{21}^{+-} \equiv 0 \equiv \rho_{21}^{-+}$ and the experimentally determined α, $\Omega_c^{\pm}$ and γ_1 of our system. The forward-propagating probe pulse is stored in the medium at $t = 2.0$ μs. Both forward and backward coupling fields are switched on simultaneously at $t = 3.2$ μs to convert the stored coherence into a SLP. Because the optical density of the medium is rather low, the probe signals leak out of the medium in both directions while the SLP is established. At $t = 5.0$ μs the SLP is converted back to a slowly forward-propagating pulse by turning off the backward coupling field. The pulse visible for $t > 5.0$ μs represents the remaining energy of the initial probe pulse after a SLP duration of 1.8 μs.

Figures 4(e) and 4(f) show the experimental data and theoretical predictions for the probe transmission through a medium of cold atoms. The timing of the coupling fields is the same as in Fig. 4(d). In Fig. 4(e) the forward and

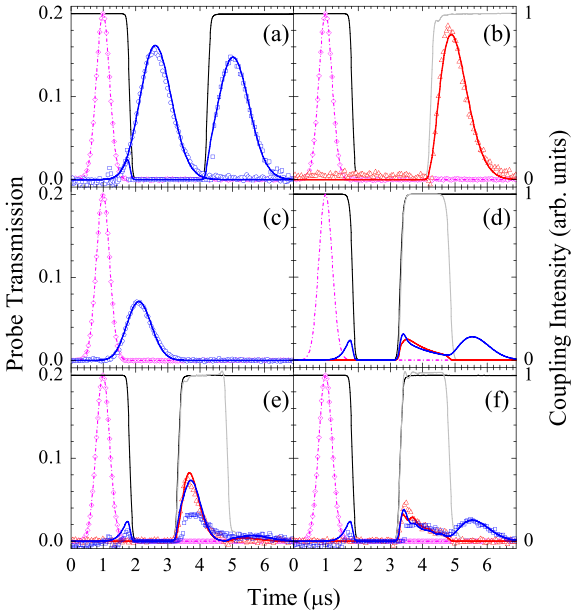

FIG. 4 (color online). Experimental data (symbols) and theoretical predictions (lines) of the probe transmission through a medium of cold atoms. (a) The output $|\Omega_p^+|^2$ (blue circles) with the constant presence of $|\Omega_c^+|^2$ (not shown) and storage and retrieval of $|\Omega_p^+|^2$ (blue squares) by $|\Omega_c^+|^2$ (black line). (b) Storage of $|\Omega_p^+|^2$ by $|\Omega_c^+|^2$ (black line) and retrieval of $|\Omega_p^-|^2$ (red triangles) by $|\Omega_c^-|^2$ (light gray line). (c) $|\Omega_p^+|^2$ (blue circles) with the constant presence of $|\Omega_c^-|^2$ (not shown). (d) Theoretical prediction of the probe transmission through a hot medium calculated with $\rho_{21}^{+-} \equiv 0 \equiv \rho_{21}^{-+}$. (e) No SLP is formed for $\Delta = 0$. (f) Formation of a SLP for $\Delta = -0.5\Gamma$. The parameters are $\Omega_c^{\pm} = 0.69\Gamma$ in (a), (b),(d),(e), and (f); $\Omega_c^- = 0.86\Gamma$ in (c); $\gamma_2 = 0.016\Gamma$ in (c),(e), and (f); $\alpha = 30$ and $\gamma_1 = 5.0 \times 10^{-4}\Gamma$ in all plots. The input $|\Omega_p^+|^2$ (magenta diamonds) is scaled down by a factor of 0.2. Because of different detection efficiencies in the forward and backward directions, the data representing the experimental $|\Omega_p^-|^2$ in (b) is scaled up by a factor of 1.4.

backward coupling frequencies are the same ($\Delta = 0$). When both coupling fields are present for 3.2 μs $\leq t \leq$ 5.0 μs two counterpropagating probe pulses are leaving the medium. There is very little observable signal for $t >$ 5.0 μs. This behavior is in agreement with the previous theoretical discussion [compare Fig. 2(c)]. The counterpropagating Raman excitations prohibit a SLP formation. In Fig. 4(f), a detuning of $\Delta = -0.5\Gamma$ is applied to the backward coupling field. We clearly observe the typical signature of a SLP formed in the medium when both coupling fields are present in good agreement with the theory and with the data shown in Fig. 3(a) of Ref. [6]. Both coupling fields are turned on long enough simultaneously that the stored light pulse could move out of the medium if no SLP were formed. This is, however, not observed. Instead, light of the SLP is leaking out of the medium showing a nearly exponential decay. Following the SLP period, a probe pulse is retrieved for $t \geq 5.0$ μs from the remaining coherence inside the medium in the forward direction. This is in clear contrast to the data shown in Fig. 4(e). The experimental data in Fig. 4(f) are also consistent with the theoretical predictions in Fig. 4(d) for a hot medium. By tuning both coupling frequencies away from each other in order to inhibit the counterpropagating Raman excitations, cold atomic media, e.g., laser-cooled atoms can be used to create SLPs as in hot media.

Next we demonstrate a new concept for SLPs that has been theoretically discussed in Refs. [8,9], according to which SLPs can be understood in terms of balanced MWM processes without a need for applying a standing-wave coupling field to form a Bragg grating. This picture of SLPs is similar to the model of matched pulses in EIT [13]. To demonstrate this concept we changed the wavelength of the backward coupling field from 780 nm to 795 nm. As shown in Fig. 1(c), the backward coupling field drove the $D1$ transition while the forward fields drove the $D2$ transition. Because of the large difference between the wavelengths of 780 and 795 nm, the forward and backward coupling fields did not form a standing wave. We repeated the same measurements as in Fig. 3 and employed the same method to determine α, $\Omega_c^{\pm}$, and γ_1. Figure 5(b) demonstrates the creation of a bichromatic SLP without a Bragg grating. As a comparison, Fig. 5(a) shows the data of a (quasi-)monochromatic SLP measured with the same setup. The measured signal at $t > 4.5$ μs is smaller than the theoretical prediction. We attribute this to an increased relaxation rate γ_1 during the formation of the SLP, because the laser field at 795 nm was not phase-locked to the fields at 780 nm. Also, as the multiorder quarter-wave plates used in the experiment were designed for 780 nm, the 795 nm backward coupling field had a worse circular polarization than the coupling field in the forward direction. For the numerical results shown in Fig. 5 we neglected the difference between the spontaneous decay rates of the excited states $|5P_{3/2}, F' = 2\rangle$ and $|5P_{1/2}, F' = 2\rangle$ and the different absorption cross sections, as the differences are only about 5% and 4%, respectively. Based on our experimental results we believe that SLPs can not only be created with two, but with an unlimited number of different wavelengths [9].

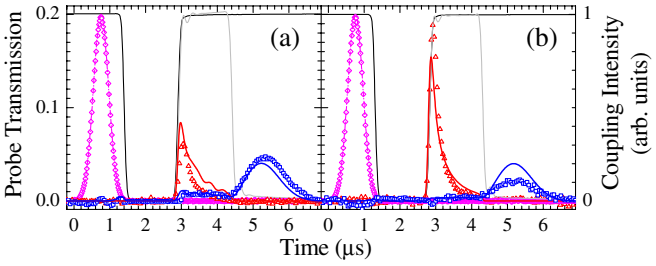

FIG. 5 (color online). Creation of a monochromatic SLP at 780 nm in (a) and a bichromatic SLP at 780 nm and 795 nm in (b). Lines, symbols, and colors are used as in Fig. 4. $\Omega_c^{\pm} = 0.77\Gamma$, $\alpha = 39$, $\gamma_1 = 7.0 \times 10^{-4}\Gamma$, $\gamma_2 = 0.016\Gamma$, and $\Delta = -0.5\Gamma$ in (a). $\Omega_c^{+} = 0.75\Gamma$, $\Omega_c^{-} = 0.77\Gamma$, $\alpha = 39$, $\gamma_1 = 4.6 \times 10^{-4}\Gamma$ with $\rho_{21}^{+-} \equiv 0 \equiv \rho_{21}^{-+}$ in (b). The input $|\Omega_p^{+}|^2$ is scaled down by a factor of 0.2. In order to plot the experimental $|\Omega_p^{-}|^2$ in (b) without having to change the vertical scale, we did not scale the experimental backward signals in (a) and (b) by a factor of 2.4 to account for different detection efficiencies in the forward and backward directions (the factor differs from the one in Fig. 4 due to a slightly changed beam alignment).

In conclusion, we have experimentally and theoretically studied SLPs in a medium of cold atoms. The experimental data are in good agreement with the theoretical predictions. Our work provides a better understanding of SLPs and opens the way to SLP studies in cold media like laser-cooled atom clouds, Bose condensates and color-center crystals, offering new possibilities for low-light-level nonlinear optics and manipulation of quantum information.

This work was supported by the National Science Council of Taiwan under Grants No. 95-2112-M-007-039-MY3 and No. 97-2628-M-007-018.

*yu@phys.nthu.edu.tw

[1] M. Fleischhauer *et al.*, Rev. Mod. Phys. **77**, 633 (2005).
[2] T. Chanelière *et al.*, Nature (London) **438**, 833 (2005).
[3] M. D. Eisaman *et al.*, Nature (London) **438**, 837 (2005).
[4] K. S. Choi *et al.*, Nature (London) **452**, 67 (2008).
[5] Q. A. Turchette *et al.*, Phys. Rev. Lett. **75**, 4710 (1995).
[6] M. Bajcsy *et al.*, Nature (London) **426**, 638 (2003).
[7] K. R. Hansen and K. Mølmer, Phys. Rev. A **75**, 053802 (2007).
[8] S. A. Moiseev and B. S. Ham, Phys. Rev. A **73**, 033812 (2006).
[9] S. A. Moiseev and B. S. Ham, Opt. Spectrosc. **103**, 210 (2007).
[10] M. Fleischhauer and M. D. Lukin, Phys. Rev. Lett. **84**, 5094 (2000).
[11] Y. W. Lin *et al.*, Opt. Express **16**, 3753 (2008).
[12] Y. F. Chen *et al.*, Phys. Rev. Lett. **96**, 043603 (2006).
[13] S. E. Harris, Phys. Rev. Lett. **70**, 552 (1993).